Mechanics of Composite Materials, Vol. 38, No. 6, 2002

INVESTIGATION OF LOCALLY LOADED MULTILAYER SHELLS BY A MIXED FINITE-ELEMENT METHOD

2. GEOMETRICALLY NONLINEAR STATEMENT

G. M. Kulikov and S. V. Plotnikova

Keywords: *multilayer shell, finite-element method, mixed model, rubber-cord composite*

Based on mixed finite-element approximations, a numerical algorithm is developed for solving linear static problems of prestressed multilayer composite shells subjected to large displacements and arbitrarily large rotations. As the sought-for functions, six displacements and eleven strains of the shell faces are chosen, which allows us to use nonlinear deformation relationships exactly representing arbitrarily large displacements of the shell as a rigid body. The stiffness matrix of a shell element has a proper rank and is calculated based on exact analytical integration. The bilinear element developed does not allow false rigid displacements and is not subjected to the membrane, shear, or Poisson locking phenomenon. The results of solving the well-known test problem on a nonsymmetrically fixed circular arch subjected to a concentrated load and the problem on a locally loaded toroidal multilayer rubber-cord shell are presented.

Introduction

In [1], an algorithm for the numerical solution of linear static problems of prestressed multilayer anisotropic Timoshenko-type shells with regard for transverse compression was constructed. The algorithm was based on a mixed TMS4 element having a number of properties useful in calculating shells subjected to loads with a high degree of localization. Since, in [1], "pure" deformation relations were used, the stiffness matrix of the shell element had six nonzero eigenvalues, which was necessary for a precise representation of small displacements of the element as a rigid body. As a result, the element did not admit false rigid displacements (mechanisms) and was not subjected to the membrane or shear locking [2, 3].

In this study, a more general algorithm for the numerical solution of geometrically nonlinear static problems of a prestressed multilayer anisotropic Timoshenko-type shell based on a mixed finite-element model (FEM) is elaborated. As a result of using nonlinear deformation relations precisely representing arbitrary large displacements of the shell as a rigid body, the stiffness matrix of the bilinear TMS4n element constructed has a proper rank. Therefore, this element, similar to its linear analog TMS4, does not admit false rigid displacements and is not subjected to the membrane, shear, or Poisson locking. The latter situation arises when the transverse compression is taken into account in the case of a predominant flexural stress state. This effect becomes more pronounced in solving problems in the geometrically nonlinear statement [4-6].

[1]For Report 1 see [1].

Tambov State Technical University, Russia. Translated from Mekhanika Kompozitnykh Materialov, Vol. 38, No. 6, pp. 815-826, November-December, 2002. Original article submitted January 28, 2002; revision submitted April 22, 2002.

The Hu–Washizu Functional

Let us supplement the Hu–Washizu functional of the geometrically nonlinear elastic theory [7] with independent approximations of displacements and strains (see Eqs. (1) and (2) in [1]). Assuming that the metrics of the shell faces $S^{\pm}$ are equivalent to the metric of the reference surface S, we come to a formula for the variation of the Hu–Washizu functional for a prestressed multilayer anisotropic shell subjected to large displacements and arbitrarily large rotations:

$$\delta J = -\iint_S \left\{ \sum_{\alpha \le i} \left[H^-_{\alpha i} - \sum_{\beta \le j} (D^{00}_{\alpha i \beta j} E^-_{\beta j} + D^{01}_{\alpha i \beta j} E^+_{\beta j}) - \underline{D^-_{\alpha i 33} E_{33}} \right] \delta E^-_{\alpha i} \right.$$

$$+ \sum_{\alpha \le i} \left[H^+_{\alpha i} - \sum_{\beta \le j} (D^{01}_{\alpha i \beta j} E^-_{\beta j} + D^{11}_{\alpha i \beta j} E^+_{\beta j}) - \underline{D^+_{\alpha i 33} E_{33}} \right] \delta E^+_{\alpha i}$$

$$+ \left[H_{33} - \sum_{\beta \le j} (D^-_{33\beta j} E^-_{\beta j} + D^+_{33\beta j} E^+_{\beta j}) - D_{3333} E_{33} \right] \delta E_{33}$$

$$+ \sum_{\alpha \le i} [(E^-_{\alpha i} - e^-_{\alpha i} - \eta^-_{\alpha i}) \delta H^-_{\alpha i} + (E^+_{\alpha i} - e^+_{\alpha i} - \eta^+_{\alpha i}) \delta H^+_{\alpha i} - H^-_{\alpha i} \delta e^-_{\alpha i} - H^+_{\alpha i} \delta e^+_{\alpha i}$$

$$- (L^-_{\alpha i} + H^-_{\alpha i}) \delta \eta^-_{\alpha i} - (L^+_{\alpha i} + H^+_{\alpha i}) \delta \eta^+_{\alpha i}] + (E_{33} - e_{33} - \eta_{33}) \delta H_{33} - H_{33} \delta e_{33}$$

$$\left. - (L_{33} + H_{33}) \delta \eta_{33} + \sum_i (p^+_i \delta v^+_i - p^-_i \delta v^-_i) \right\} A_1 A_2 \, d\alpha_1 d\alpha_2$$

$$- \oint_\Gamma (\hat{H}^-_{\nu\nu} \delta v^-_\nu + \hat{H}^+_{\nu\nu} \delta v^+_\nu + \hat{H}^-_{\nu t} \delta v^-_t + \hat{H}^+_{\nu t} \delta v^+_t + \hat{H}^-_{\nu 3} \delta v^-_3 + \hat{H}^+_{\nu 3} \delta v^+_3) \, ds. \tag{1}$$

The designations used hereinafter correspond to those utilized in [1]: $e^{\pm}_{\alpha i}, e_{33}$ and $\eta^{\pm}_{\alpha i}, \eta_{33}$ are the linear and nonlinear components of the Green–Lagrange strain tensor (see Eqs. (4) in [1]) and the index variables are $i, j, l, m = 1, 2, 3$ and $\alpha, \beta, \gamma = 1, 2$. However, in this case, contrary to [1], the resultants of stresses have a different mechanical meaning: $H^{\pm}_{\alpha i}$ and H_{33} are the resultants of the Piola–Kirchhoff symmetric stress tensor and $L^{\pm}_{\alpha i}$ and L_{33} are the resultants of the Cauchy tensor of initial stresses, which are determined by the formulas

$$H^{\pm}_{\alpha i} = \sum_{k=1}^{N} \int_{\delta_{k-1}}^{\delta_k} S^{(k)}_{\alpha i} N^{\pm}(\alpha_3) \, d\alpha_3, \quad H_{33} = \sum_{k=1}^{N} \int_{\delta_{k-1}}^{\delta_k} S^{(k)}_{33} \, d\alpha_3,$$

$$L^{\pm}_{\alpha i} = \sum_{k=1}^{N} \int_{\delta_{k-1}}^{\delta_k} \tau^{(k)}_{\alpha i} N^{\pm}(\alpha_3) \, d\alpha_3, \quad L_{33} = \sum_{k=1}^{N} \int_{\delta_{k-1}}^{\delta_k} \tau^{(k)}_{33} \, d\alpha_3,$$

where $N^{\pm}(\alpha_3)$ are symmetric shape functions [1].

The components of the Piola–Kirchhoff stress tensor may be calculated by the complete relationships of the generalized Hooke's law

$$S^{(k)}_{ij} = \sum_{l,m} b^{(k)}_{ijlm} \varepsilon_{lm}, \quad b^{(k)}_{\alpha\beta\gamma 3} = b^{(k)}_{\alpha 333} = 0,$$

where $b_{ijlm}^{(k)}$ are the stiffnesses of a kth layer of the shell. However, to calculate shells of incompressible or nearly incompressible materials with the Poisson ratios of the layers close to 0.5 [8] and also to exclude the Poisson locking [6], we must assume approximately that $b_{\alpha\beta 33}^{(k)} = 0$. This means that the underlined terms in the formula for the variation of Hu–Washizu functional (1) can be omitted [1], since

$$D_{\alpha\beta 33}^{\pm} = \sum_{k=1}^{N} \int_{\delta_{k-1}}^{\delta_k} b_{\alpha\beta 33}^{(k)} N^{\pm}(\alpha_3)\, d\alpha_3 .$$

We should note that functional (1) generalizes the respective Hu–Washizu functionals of multilayer shells given in [1, 9, 10].

Numerical Solution Algorithm for Geometrically Nonlinear Static Problems of Multilayer Anisotropic Shells

Let us consider the problem of local loading of a prestressed multilayer anisotropic shell in the geometrically nonlinear statement. It can be proved [9, 10] that the nonlinear deformation relations used precisely represent arbitrary large displacements of the shell as a rigid body. This is of principal importance in calculating shells with a high degree of localization of a load, including shells subjected to concentrated actions.

Let us present the variation of Hu–Washizu functional (1) in the matrix form

$$\delta J^{el} = -\int_{-1}^{1}\int_{-1}^{1} [(\mathbf{H}-\mathbf{DE})^{\mathrm{T}}\delta\mathbf{E} + (\mathbf{E}-\mathbf{e}-\acute{\mathbf{A}})^{\mathrm{T}}\delta\mathbf{H} - \mathbf{H}^{\mathrm{T}}\delta\mathbf{e} - (\mathbf{L}+\mathbf{H})^{\mathrm{T}}\delta\acute{\mathbf{A}} + \mathbf{P}^{\mathrm{T}}\delta\mathbf{v}]\,\Lambda d\xi_1 d\xi_2 - \oint_{\Gamma^{el}} \hat{\mathbf{H}}_{\Gamma}^{\mathrm{T}}\delta\mathbf{v}_{\Gamma}\, ds,*,$$

$$\mathbf{v} = [v_1^- \; v_1^+ \; v_2^- \; v_2^+ \; v_3^- \; v_3^+]^{\mathrm{T}}, \quad \mathbf{v}_{\Gamma} = [v_{\nu}^- \; v_{\nu}^+ \; v_t^- \; v_t^+ \; v_3^- \; v_3^+]^{\mathrm{T}},$$

$$\mathbf{P} = [-p_1^- \; p_1^+ \; -p_2^- \; p_2^+ \; -p_3^- \; p_3^+]^{\mathrm{T}}, \quad \hat{\mathbf{H}}_{\Gamma} = [\hat{H}_{\nu\nu}^- \; \hat{H}_{\nu\nu}^+ \; \hat{H}_{\nu t}^- \; \hat{H}_{\nu t}^+ \; \hat{H}_{\nu 3}^- \; \hat{H}_{\nu 3}^+]^{\mathrm{T}}, \tag{2}$$

$$\mathbf{e} = [e_{11}^- \; e_{11}^+ \; e_{22}^- \; e_{22}^+ \; e_{12}^- \; e_{12}^+ \; e_{13}^- \; e_{13}^+ \; e_{23}^- \; e_{23}^+ \; e_{33}]^{\mathrm{T}}, \quad \acute{\mathbf{A}} = [\eta_{11}^- \; \eta_{11}^+ \; \eta_{22}^- \; \eta_{22}^+ \; \eta_{12}^- \; \eta_{12}^+ \; \eta_{13}^- \; \eta_{13}^+ \; \eta_{23}^- \; \eta_{23}^+ \; \eta_{33}]^{\mathrm{T}},$$

$$\mathbf{E} = [E_{11}^- \; E_{11}^+ \; E_{22}^- \; E_{22}^+ \; E_{12}^- \; E_{12}^+ \; E_{13}^- \; E_{13}^+ \; E_{23}^- \; E_{23}^+ \; E_{33}]^{\mathrm{T}}, \quad \mathbf{H} = [H_{11}^- \; H_{11}^+ \; H_{22}^- \; H_{22}^+ \; H_{12}^- \; H_{12}^+ \; H_{13}^- \; H_{13}^+ \; H_{23}^- \; H_{23}^+ \; H_{33}]^{\mathrm{T}},$$

$$\mathbf{L} = [L_{11}^- \; L_{11}^+ \; L_{22}^- \; L_{22}^+ \; L_{12}^- \; L_{12}^+ \; L_{13}^- \; L_{13}^+ \; L_{23}^- \; L_{23}^+ \; L_{33}]^{\mathrm{T}},$$

where ξ_1 and ξ_2 are the local coordinates of a shell element, $\Lambda(\xi_1, \xi_2)$ is the function describing the metric of the element, $\mathbf{v}$ is the displacement vector, $\mathbf{v}_{\Gamma}$ is the displacement vector of the boundary contour Γ^{el} of the element, $\mathbf{E}$, $\mathbf{e}$, and $\acute{\mathbf{A}}$ are vectors characterizing the deformation relations, $\mathbf{H}$ is the resultant vector of Piola–Kirchhoff stresses, $\mathbf{L}$ is the resultant vector of initial Cauchy stresses, $\hat{\mathbf{H}}_{\Gamma}$ is the resultant vector of loads acting on the boundary Γ^{el} of the element, $\mathbf{P}$ is the vector of surface loads, and $\mathbf{D}$ is an asymmetric 11×11 matrix of elastic coefficients, whose elements are determined according to [1].

Since the vectors $\mathbf{v}$, $\mathbf{E}$, and $\mathbf{H}$ in functional (2) are independent functional variables, independent approximations must be used for them on the element considered. For the displacements, we use the standard bilinear approximation

$$\mathbf{v} = \sum_{r} N_r \mathbf{v}_r, \tag{3}$$

where $N_r(\xi_1, \xi_2)$ are linear shape functions and $\mathbf{v}_r = [v_{1r}^- \; v_{1r}^+ \; v_{2r}^- \; v_{2r}^+ \; v_{3r}^- \; v_{3r}^+]^{\mathrm{T}}$ are the vectors of nodal displacements ($r = \overline{1,4}$). For the strains and resulting stresses, according to the method of double approximation [11-13] generalized to the case of transverse compression, we have even simpler formulas:

$$\mathbf{E}=\sum_{r_1,r_2}\mathbf{Q}^{r_1r_2}\mathbf{E}^{r_1r_2}\xi_1^{r_1}\xi_2^{r_2},$$

$$\mathbf{E}^{00}=[E_{11}^{-00}\ E_{11}^{+00}\ E_{22}^{-00}\ E_{22}^{+00}\ E_{12}^{-00}\ E_{12}^{+00}\ E_{13}^{-00}\ E_{13}^{+00}\ E_{23}^{-00}\ E_{23}^{+00}\ E_{33}^{00}]^{\mathrm{T}},$$

$$\mathbf{E}^{01}=[E_{11}^{-01}\ E_{11}^{+01}\ E_{13}^{-01}\ E_{13}^{+01}\ E_{33}^{01}]^{\mathrm{T}},\ \mathbf{E}^{10}=[E_{22}^{-10}\ E_{22}^{+10}\ E_{23}^{-10}\ E_{23}^{+10}\ E_{33}^{10}]^{\mathrm{T}},\ \mathbf{E}^{11}=[E_{33}^{11}], \tag{4a}$$

$$\mathbf{H}=\sum_{r_1,r_2}\mathbf{Q}^{r_1r_2}\mathbf{H}^{r_1r_2}\xi_1^{r_1}\xi_2^{r_2},\quad \mathbf{L}=\sum_{r_1,r_2}\mathbf{Q}^{r_1r_2}\mathbf{L}^{r_1r_2}\xi_1^{r_1}\xi_2^{r_2}, \tag{4b}$$

where $\mathbf{E}^{00}$ is the vector characterizing homogeneous deformation shapes, $\mathbf{E}^{01}$, $\mathbf{E}^{10}$, and $\mathbf{E}^{11}$ are the vectors characterizing higher deformation shapes, $\mathbf{Q}^{00}$ is an 11×11 unit matrix, $\mathbf{Q}^{01}$ and $\mathbf{Q}^{10}$ are 11×5 matrices, and $\mathbf{Q}^{11}$ is an 11×1 matrix, all introduced in [1] for a more compact representation of the resolving matrix equations. The meaning of the vectors $\mathbf{H}^{r_1r_2}$ and $\mathbf{L}^{r_1r_2}$ is similar to that of $\mathbf{E}^{r_1r_2}$. Hereinafter, $r_1, r_2 = 0, 1$.

Introducing displacements (3), strains (4a), and resulting stresses (4b) into Eq. (2) and using the standard variational procedure, we obtain the following nonlinear equations of a mixed FEM model:

$$\mathbf{E}^{r_1r_2}=(\mathbf{Q}^{r_1r_2})^{\mathrm{T}}(\mathbf{B}^{r_1r_2}+\mathbf{R}^{r_1r_2}\mathbf{u})\mathbf{u},\quad \mathbf{H}^{r_1r_2}=(\mathbf{Q}^{r_1r_2})^{\mathrm{T}}\mathbf{D}\mathbf{Q}^{r_1r_2}\mathbf{E}^{r_1r_2},$$

$$\sum_{r_1,r_2}\frac{1}{3^{r_1+r_2}}[(\mathbf{B}^{r_1r_2}+2\mathbf{R}^{r_1r_2}\mathbf{u})^{\mathrm{T}}\mathbf{Q}^{r_1r_2}\mathbf{H}^{r_1r_2}+2(\mathbf{R}^{r_1r_2}\mathbf{u})^{\mathrm{T}}\mathbf{Q}^{r_1r_2}\mathbf{L}^{r_1r_2}]=\mathbf{F}, \tag{5}$$

where $\mathbf{u}=[\mathbf{v}_1^{\mathrm{T}}\ \mathbf{v}_2^{\mathrm{T}}\ \mathbf{v}_3^{\mathrm{T}}\ \mathbf{v}_4^{\mathrm{T}}]^{\mathrm{T}}$ is the vector of nodal displacements of the shell element, $\mathbf{F}$ is the vector of nodal loads, $\mathbf{B}^{r_1r_2}$ are 11×24 deformation matrices corresponding to the linear components of the strain tensor, $\mathbf{R}^{r_1r_2}$ are three-dimensional $11\times 24\times 24$ deformation arrays corresponding to the nonlinear components of the strain tensor. In this case, $\mathbf{R}^{r_1r_2}\mathbf{u}$ are 11×24 matrices whose elements are calculated from the formulas

$$(\mathbf{R}^{r_1r_2}\mathbf{u})_{\mathrm{pq}}=\sum_s R_{pqs}^{r_1r_2}u_s\quad (p=\overline{1,11};\ q,s=\overline{1,24}).$$

Excluding the vectors $\mathbf{E}^{r_1r_2}$ and $\mathbf{H}^{r_1r_2}$ from Eqs. (5) and taking into account the relation

$$\mathbf{D}^{r_1r_2}=\mathbf{Q}^{r_1r_2}(\mathbf{Q}^{r_1r_2})^{\mathrm{T}}\mathbf{D}\mathbf{Q}^{r_1r_2}(\mathbf{Q}^{r_1r_2})^{\mathrm{T}},$$

we obtain the resolving matrix equation of equilibrium of the shell element

$$\mathbf{G}(\mathbf{u})=\mathbf{F}, \tag{6}$$

where

$$\mathbf{G}(\mathbf{u})=\sum_{r_1,r_2}\frac{1}{3^{r_1+r_2}}[(\mathbf{B}^{r_1r_2}+2\mathbf{R}^{r_1r_2}\mathbf{u})^{\mathrm{T}}\mathbf{D}^{r_1r_2}(\mathbf{B}^{r_1r_2}+\mathbf{R}^{r_1r_2}\mathbf{u})\mathbf{u}+2(\mathbf{R}^{r_1r_2}\mathbf{u})^{\mathrm{T}}\mathbf{Q}^{r_1r_2}\mathbf{L}^{r_1r_2}].$$

According to [10], from Eqs. (5), we can easily derive the relations

$$hE_{33}^{10}=A_1\bar{\xi}_1(E_{13}^{+00}-E_{13}^{-00}),\quad hE_{33}^{01}=A_2\bar{\xi}_2(E_{23}^{+00}-E_{23}^{-00}),$$

$$hE_{33}^{11}=A_1\bar{\xi}_1(E_{13}^{+01}-E_{13}^{-01}),\quad hE_{33}^{11}=A_2\bar{\xi}_2(E_{23}^{+10}-E_{23}^{-10}), \tag{7}$$

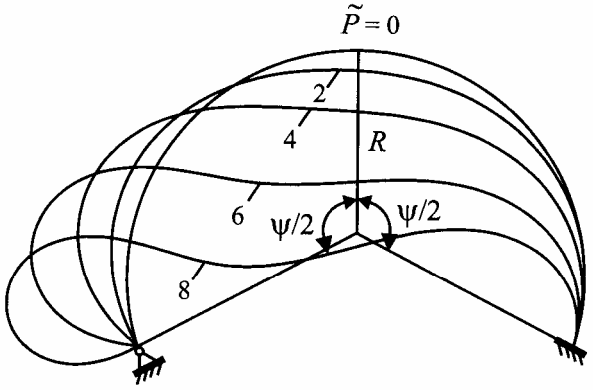

Fig.1. Scheme of a circular arch.

TABLE 1. Displacements $\bar{v}_i = (v_i^- + v_i^+)/2$ of a Circular Arch at the Force Application Point

Force, $\widetilde{p}$	Study [14]		TMS4n				Number of iterations
			Equations (8)		Equations (9)		
	$-\bar{v}_1$	$-\bar{v}_3$	$-\bar{v}_1$	$-\bar{v}_3$	$-\bar{v}_1$	$-\bar{v}_3$	
2	6.75	8.61	6.84	8.64	6.59	8.44	10
4	21.53	25.70	21.73	25.82	21.17	25.24	16
6	43.11	58.21	43.35	58.60	42.86	57.74	25
8	56.01	93.63	56.40	94.76	55.96	93.74	40

which mean that only seven higher approximation forms of strains (for example, E_{11}^{-01}, E_{11}^{+01}, E_{22}^{-10}, E_{22}^{+10}, E_{13}^{-01}, E_{13}^{+01}, and E_{23}^{-10}) among the eleven ones introduced according to Eqs. (4a) are independent. Relations (7) ensure the necessary number of degrees of freedoms needed for a precise representation of large displacements of the shell element as a rigid body. It should be noted that the stiffness matrix of the element is calculated based on precise analytical integration. As a result, we managed to construct a universal and very efficient element TMS4n, which does not admit false displacements (mechanisms) and is not subjected to the Poisson locking.

Equation (6) is nonlinear and can be solved by the Newton–Raphson method

$$\mathbf{u}^{[n+1]} = \mathbf{u}^{[n]} + \left[\frac{\partial \mathbf{G}}{\partial \mathbf{u}}(\mathbf{u}^{[n]})\right]^{-1} [\mathbf{F} - \mathbf{G}(\mathbf{u}^{[n]})],$$

where $n = 0.\ 1, \ldots$. The iterations are continued until the inequality

$$||\mathbf{U}^{[n+1]} - \mathbf{U}^{[n]}|| < \varepsilon ||\mathbf{U}^{[n]}||,$$

is fulfilled, where $\mathbf{U}$ is the global vector of nodal displacements, $||\bullet||$ is the Euclidean norm in the space of displacements, and ε is the calculation accuracy specified a priori.

The nonlinear TMS4n element served as the basis for the TIRANA (Tire Analysis) software package intended for use in tire industry in designing resin-cord composites, in particular, pneumatic tires. The results of test calculations show a high accuracy and efficiency of the TMS4n element.

TABLE 2. Deflection of the Tire at the Center of the Loading Area

Loading cases	I	II	III	IV	[16]
c	0	$q_0/3$	$2q_0/3$	q_0	
d	q_0	$q_0/2$	0	$-q_0/2$	
$v_3^+(0, 0)$, mm	30.2	28.5	17.8	16.8	18.0

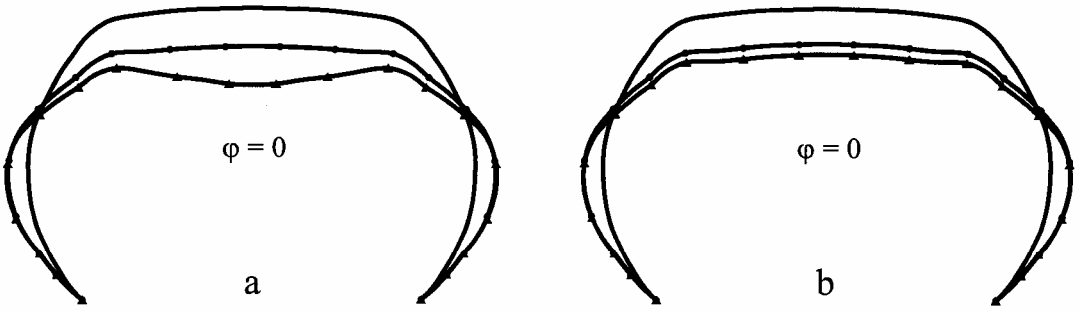

Fig. 2. Deformed profiles of a 175/70R13 tire subjected to internal pressure (——) and to an additional local load in the linear (—●—) and nonlinear (—▲—) statements: loading case I (a) and loading case III (b).

Numerical Results and Discussion

As a first example, we will consider a circular arch under the action of a concentrated force $\widetilde{P} = 12PR^2/Ebh^3$ at its top (Fig. 1). Let the left-hand end of the arch be hinge-supported and the right-hand one fixed. The arch has the following mechanogeometrical characteristics [7]: $E = 2\cdot 10^6$, $\nu = 0$, $R = 100$, $b = 6$, $h = 1$, and $\psi = 215°$. This problem has attracted the attention of many researches from the viewpoint of studying the asymmetric transient buckling of the arch subjected to large displacements and large rotations. However, this problem is not considered here, since we were interested in the ability of the TMS4n element to adequately describe large displacements and large rotations of the arch without invoking the incremental approach [15].

The solution results of the problem were obtained for two cases of hinge support of the left-hand edge:

$$v_1^- = v_3^- = 0, \tag{8}$$

$$v_1^+ = v_3^+ = 0 \tag{9}$$

and are shown in Table 1. For comparison, we have also presented there the results of calculation [14] with the use of the FEM in the form of the method of displacements based on the geometrically nonlinear Timoshenko-type shell theory, without account of transverse compression but with regard for transverse normal stresses. It is seen that these data agree well with one another. We should note that the results of this study were obtained without the use of the incremental approach and the number of iterations necessary for reaching the given accuracy $\varepsilon = 10^{-6}$ is indicated in Table 1. Additionally, Fig. 1 shows four deformed configurations of the arch before its transient buckling at $\widetilde{P} = 9.14$ [14].

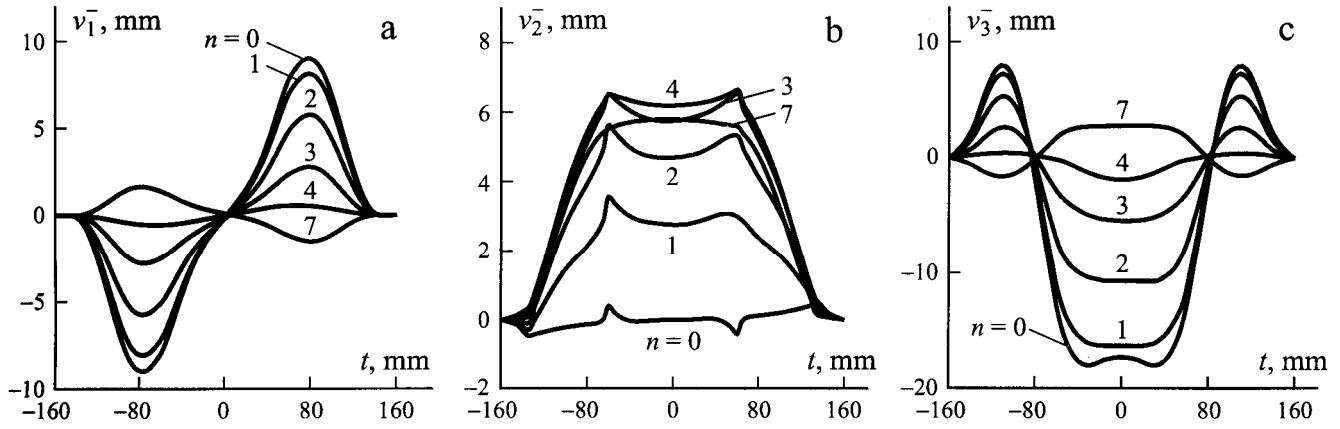

Fig. 3. Displacements v_i^- of the inner surface of a 175/70R13 tire vs. the meridional coordinate t for $\varphi = n\pi/20$: v_1^- (a), v_2^- (b), and v_3^- (c).

Let us consider the geometrically nonlinear problem of local loading of a 175/70R13 radial car tire (see Fig. 3 in [1]). First, the tire was subjected to an internal pressure of $p = 0.2$ MPa. Then, for the prestressed rubber-cord shell subjected to the conservative load

$$q_n^+ = -c - d\sqrt{1 - \frac{t^2}{a^2} - \frac{\varphi^2}{\Delta^2}}, \quad \frac{t^2}{a^2} + \frac{\varphi^2}{\Delta^2} \le 1, \tag{10}$$

in the direction perpendicular to the rotation axis [1], we solved the geometrically nonlinear problem. As in [1], four types of local loads modeling the contact pressure and distributed inside an ellipse with semiaxes $a = 50$ mm and $\Delta = \pi/10$ rad were considered, where t and φ are the meridional and circumferential coordinates of the tire. The values of the coefficients c and d of Eq. (10) are given in Table 2 ($q_0 = 0.333$ MPa). It should be noted that the resulting compressive force was the same for all loads and was equal to 3 kN. In our numerical calculations, we assumed that the edges of the tire with the coordinates $t = \pm 160$ mm were rigidly fixed.

The calculation results for the deformed profile of the external contour of the tire at $\varphi = 0$, for loading cases I and III, are shown in Fig. 2. A comparison with the results for the linear problem from [1] is also given. In addition, Table 2 shows deflections of the tire at the center of the loading area for all the four loads considered and the experimental data from [16]. As is seen, the results of calculating the deformed profiles of the tire in the geometrically nonlinear statement for loading cases I and II are unacceptable because of the highly overestimated values of the deflections. The reason is that, in these cases, the loads modeling the distribution of the contact pressure differ from their actual distribution considerably. The solution of the problem in the linear statement shows that the deformed profiles of the tire are practically the same for all loading types [1].

To make the picture more complete, we also elucidated the effect of anisotropy on the deformed state of a tire with a breaker containing two angle-ply resin-cord layers reinforced at ±70° angles to the meridian [17]. Figure 3 shows displacements of the inner surface of the tire as functions of the meridional coordinate for loading type III and some values of the circumferential coordinate $\varphi = n\pi/20$, where $n = 0, 1, 2, 3, 4, 7$. On the whole, the effect of anisotropy on the distribution of the displacements v_1^- and v_3^- is barely noticeable. On the contrary, the circumferential displacement v_2^-, which is comparable in magnitude with the meridional displacement v_1^-, is distributed at $\varphi = \pi/20$ and $\varphi = \pi/10$ in a rather intricate manner, with a noticeable disturbance of the conditions of symmetry and antisymmetry.

Acknowledgments. The authors express their gratitude to the reviewer for constructive remarks, which favored the improvement of the manuscript considerably.

REFERENCES

1. G. M. Kulikov and S. V. Plotnikova, "Investigation of locally loaded multilayer shells by a mixed finite-element method. 1. Geometrically linear statement," Mech. Compos. Mater., **38**, No. 5, 397-496 (2002).
2. A. N. Golovanov and M. S. Kornishin, Introduction to the Finite-Element Method for the Statics of Thin Shells [in Russian], KFTI Akad. Nauk SSSR, Kazan' (1989).
3. R. B. Rikards, Finite-Element Method in the Theory of Shells and Plates [in Russian], Zinatne, Riga (1988).
4. P. Betsch, F. Gruttmann, and E. Stein, "A 4-node finite shell element for the implementation of general hyperelastic 3D-elasticity at finite strains," Comput. Meth. Appl. Mech. Eng., **130**, 57-79 (1996).
5. Y. Basar, M. Itskov, and A. Eckstein, "Composite laminates: nonlinear interlaminar stress analysis by multi-layer shell elements," Comput. Meth. Appl. Mech. Eng., **185**, 367-397 (2000).
6. M. Bischoff and E. Ramm, "On the physical significance of higher order kinematic and static variables in a three-dimensional shell formulation," Int. J. Solids Struct., **37**, 6933-6960 (2000).
7. K. Washizu, Variational Methods in Elasticity and Plasticity, Pergamon Press, Oxford (1975).
8. G. M. Kulikov and S. V. Plotnikova, "Comparative analysis of two algorithms for numerical solution of nonlinear static problems for multilayered anisotropic shells of revolution. 2. Account of transverse compression," Mech. Compos. Mater., **35**, No. 4, 293-300 (1999).
9. G. M. Kulikov and S. V. Plotnikova, "Finite-element formulation of straight composite beams undergoing finite rotations," Trans. TSTU, **7**, 617-633 (2001).
10. G. M. Kulikov and S. V. Plotnikova, "Simple and effective elements based upon Timoshenko–Mindlin shell theory," Comput. Meth. Appl. Mech. Eng., **191**, 1173-1187 (2002).
11. A. S. Sakharov and I. Altenbach (eds.), Finite-Element Method in Mechanics of Solid Bodies [in Russian], Vishcha Shkola, Kiev (1982).
12. T. J. R. Hughes and T. E. Tezduyar, "Finite elements based upon Mindlin plate theory with particular reference to the four-node bilinear isoparametric element," Trans. ASME, J. Appl. Mech., **48**, 587-596 (1981).
13. G. Wempner, D. Talaslidis, and C. M. Hwang, "A simple and efficient approximation of shells via finite quadrilateral elements," Trans. ASME, J. Appl. Mech., **49**, 115-120 (1982).
14. M. Li, "The finite deformation theory for beam, plate and shell. Part I. The two-dimensional beam theory," Comput. Meth. Appl. Mech. Eng., **146**, 53-63 (1997).
15. K. J. Bathe, Finite Element Procedures, Prentice Hall, New York (1996).
16. A. E. Belkin, B. L. Bukhin, O. N. Mukhin, and N. L. Narskaya, "Some models and methods of pneumatic tire mechanics," in: F. Böhm and H. P. Willumeit (eds.), Tyre Models for Vehicle Dynamic Analysis (1997), pp. 250-271.
17. E. I. Grigolyuk and G. M. Kulikov, Multilayer Reinforced Shells. Calculation of Pneumatic Tires [in Russian], Mashinostroenie, Moscow (1988).